JOURNAL OF MATERIALS SCIENCE 23 (1988) 2281–2293

Review
Polymer optical fibres

CHRISTOPHER EMSLIE
Department of Electronics and Computer Science, University of Southampton Optical Fibre Group, Southampton SO9 5NH, UK

The background to the development of polymer optical fibres (POFs) and the methods used for their manufacture are described. The optical properties of polymers are then discussed in the context of fibres, taking the most common POF materials, polymethylmethacrylate and polystyrene, as examples. The poor market penetration of POFs, due to inadequate performance in terms of attenuation, bandwidth and temperature resistance, is then explained. The article concludes with a discussion of techniques which show great promise for the development of a new generation of high-performance POFs which will satisfy market demands.

Nomenclature

n_1, n_2	Refractive indices of core and cladding
θ_A	Acceptance angle
τ	Turbidity
$\tau_{(LSO)}$	Isotropic turbidity
λ	Wavelength
ϱ	Density
ε	Dielectric constant
T	Temperature
T_f	Fictive temperature
T_g	Glass transition temperature
k	Boltzmann constant
β_T	Isothermal compressibility
C_u	Cabannes factor
ϱ_u	Depolarization factor
α_e	Ultraviolet absorption loss ($dB\,km^{-1}$)
ν	Frequency
K	Interatomic force constant
μ	Reduced mass
m_1, m_2	Mass
δt_s	Delay time
c	Velocity of light
β_t	Bit-rate

1. Introduction

Although inorganic glasses remain unsurpassed as guided-wave media, they are not universally ideal materials for the production of optical fibres. Their low elastic limits dictate that the remarkable flexibility, characteristic of optical fibres, may only be observed in those of very small diameter, typically 125 μm. The inherent brittleness of glass requires that a more elastic polymer coating be applied to the fibre to protect its surface and prevent the growth of Griffiths cracks [1] and consequent fracture.

The small diameter of the fibres, although advantageous in its saving of both space and weight, does create handling problems in some applications. In particular, the engineering solutions to the problems of fibre connection [2] are relatively complex and time-consuming, thus contributing significantly to the cost of some systems. In addition, in many environments fibres are vulnerable to both impact and abrasion damage and thus require further protective sheathing; a suitably protected, single fibre cable is shown in Fig. 1a.

In direct contrast, although the optical transparency of polymer glasses is poor, due to their molecular structure, their elastic limits are high. In particular polymethylmethacrylate (PMMA) may withstand recoverable strains of 13% [3], with 6% possible in even the more brittle polymer glasses such as polystyrene (PS). Furthermore, it has been demonstrated, both by Rehage and Goldbach [4] (in the case of PMMA) and Haward *et al.* (PS) [5], that by pre-orientation of the polymer molecules, yield phenomena such as crazing [6–9] may be suppressed and elasticity further increased. It is this high elasticity which allows the fabrication of tough and flexible polymer optical fibres (POFs) with diameters of up to one millimetre. Such large-diameter fibres are easier to align, joint and handle generally than their 125 μm, silica-based counterparts. The inherent and induced toughness of the materials also helps to reduce cabling requirements, and consequently the overall cost and weight; a simple extruded polyethylene jacket suffices for many applications. A typical POF cable is shown in Fig. 1b.

Ease of jointing is also facilitated by the high numerical apertures (NA) of POFs which can be obtained because polymers are available over a wide range of refractive indices. These indices vary from 1.32, for highly fluorinated acrylic-based materials, to around 1.6 for some cast phenolic resins. The NA is defined by the equation

$$\mathrm{NA} = (n_1^2 - n_2^2)^{1/2} = \sin(\theta_A/2) \qquad (1)$$

Thus, it represents both the difference in refractive index between the core and the cladding and, by defining acceptance angle θ_A (Fig. 2), the light-gathering ability of the fibre. A typical POF has an NA of

0022–2461/88 $03.00 + .12

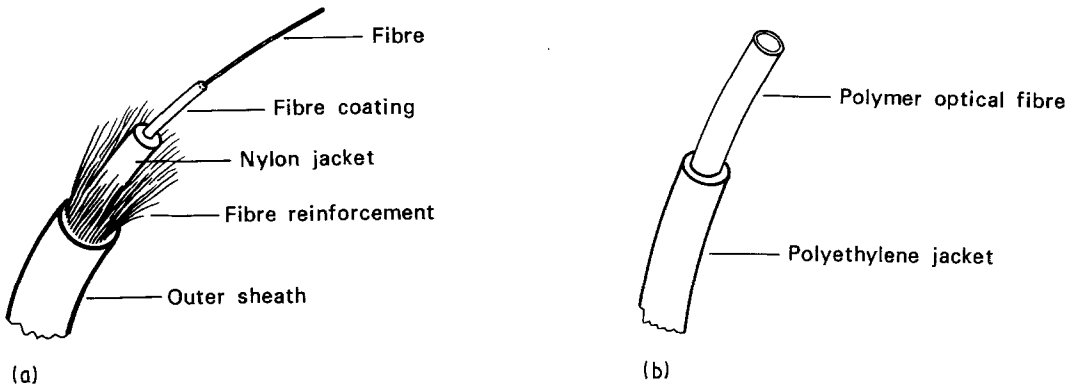

Figure 1 (a) A conventional single fibre cable. (b) A single POF cable.

around 0.5, resulting in an acceptance angle of 60°, compared with 0.14 and 16° for a comparable silica-based fibre.

The large acceptance angle greatly eases the alignment tolerances in POF connectors which, in turn, greatly reduces their complexity. Thus, connectors may be produced from thermoplastics by the high-volume, low-precision technique of injection-moulding [10]. The consequent low price and simplicity of operation of such devices further reduces the overall cost of high connector density systems. A typical POF connector is shown in Fig. 3.

Thus, polymers could offer significant advantages over silica in short-distance data transmission systems, such as local area networks (LANs) and those found in aircraft and automobiles, where ease of handling and installation are more important than optical attenuation.

2. Historical background

Throughout the 1970s two companies worked on the commercial development of POFs; duPont in the United States and Mitsubishi Rayon in Japan. In 1974, Mitsubishi filed a patent [11] covering the melt-spinning of a simple light-guiding core–cladding structure such as that shown in Fig. 2. PMMA or PS was employed as the core material and various fluorinated polymers as cladding. The minimum attenuation quoted was 3500 dB km^{-1} at an unspecified wavelength. Later in the same year they patented their continuous casting process for high-purity acrylics [12] which has since led to the development of Eska™. This is a PMMA-core, poly(fluoroalkylmethacrylate)-cladded fibre which now dominates the market for POFs. The current, premium grade of Eska (Eska Extra) has minimum losses quoted as 125 dB km^{-1} at 567 nm.

At duPont, in the mid-1970s, Schleinitz [13] demonstrated that the toughness of PMMA-core fibres could be increased by molecular orientation and he reported losses below 300 dB km^{-1} at 567 nm. He then went on to show that the minimum loss could be reduced below 200 dB km^{-1} at the increased wavelength of 690 nm by the use of deuterated PMMA (PMMA-D8).

It was losses such as these which stimulated serious interest in POFs as data-transmission media rather than as the simple, ornamental or display-quality light guides initially envisaged. The duPont work is well reported in the patent literature [14, 15] and was commercialized as the Crofon™ [16] series of fibres. However, duPont have since gradually withdrawn from the market.

Since the early 1980s, the driving force behind further developments in the field of POFs has been the work of Kaino and co-workers [17–22] at NTT's Ibaraki laboratories. Their work has brought about the reduction of the losses of PMMA-core fibres to 55 dB km^{-1} [22] (567 nm) and those of PMMA-D8-core fibres to 20 dB km^{-1} [21] (680 nm).

3. Fabrication techniques

3.1. Bulk polymerization

Light-scattering caused by the presence of particulate matter within the core is a major potential source of loss in optical fibres [23]. The need to minimize this optical loss places severe restrictions on the suitability of polymerization techniques which, in turn, limit the choice of polymer.

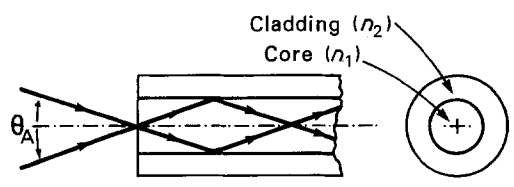

Figure 2 The waveguide structure of an optical fibre; $n_1 > n_2$.

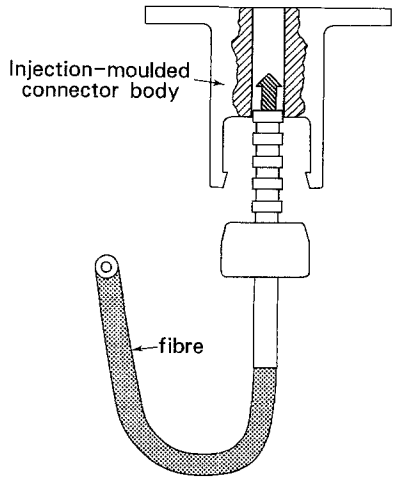

Figure 3 A typical POF connector.

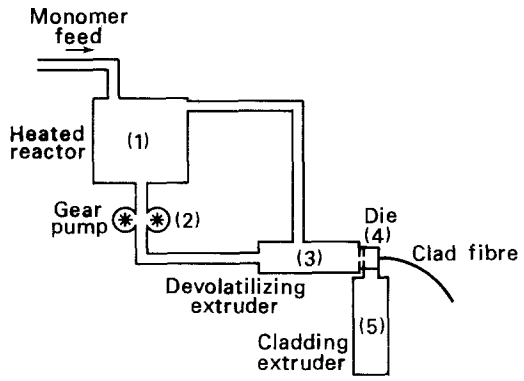

Figure 4 A schematic representation of a continuous extrusion process.

The susceptibility of a polymerization process to particulate contamination depends upon two main factors; the required additives and the total surface area of the final product. The additives themselves may bear particulate matter and the large surface area of a powdered product may become contaminated far more easily than, for example, a solid block of the material. Thus, common commercial techniques, for example emulsion polymerization [24], which both requires the dispersal of the monomer in another liquid and produces a granular polymer product, are unattractive as methods for the synthesis of low-loss materials for POFs.

Bulk polymerization [24], in which monomer is polymerized with only minute amounts of additives, is a process more suited to high purity and thus has been that preferred for the fabrication of POFs. For this method to be possible, the monomer must be an efficient solvent of its polymer. Thus, the polymer forms in a "syrup" which becomes more viscous as the reaction progresses, and the concentration of polymer in monomer increases. Eventually a solid mass of pure polymer is produced. This proviso effectively excludes whole families of materials, including well-known polymer glasses such as polyvinylchloride (PVC) and polycarbonate (PC). In practice, choice is restricted to PMMA, PS and polymers closely related to them; all published research has been concentrated on these materials.

Of the three production processes outlined, continuous and batch-extrusion are developments of conventional polymer-processing techniques, whereas preform drawing has been adapted from the silica fibre industry. All employ bulk polymerization for the core materials.

3.2. Continuous extrusion

A schematic diagram of a continuous extrusion process, such as that employed by Mitsubishi Rayon [11, 12] for the production of Eska, is shown in Fig. 4. The essential characteristic of this process is that monomer, containing traces of polymerization initiator and chain transfer agent (molecular weight modifier), may be continuously fed to the reactor (1) and clad fibre continuously withdrawn from the die (4). Thus it is an ideal commercial process since high production rates are possible.

The temperature of the reactor and quantities of initiator and chain transfer agent in the feed are allied to the fibre production rate in such a way as to maintain the proportion of polymer to monomer, within the reactor, at between 60 and 80%. At typical reactor temperatures of around 150° C, this concentrated solution (or syrup) flows easily and may be pumped from the reactor to the devolatilizing extruder (3) by means of the gear-pump (2). The devolatilizing extruder is engineered to subject this polymer–monomer solution to a rapid reduction in pressure which causes the excess monomer to evaporate and be recycled to the reactor. Thus, the polymer which reaches the die (4) contains less than 1% monomer. Upon emerging from the die, the core-polymer is clad immediately with a second polymer by means of another extruder (5).

Maintaining the conversion of monomer to polymer well below 100% has two distinct advantages: reduced processing temperature and increased reaction rate. The presence of the monomer plasticizes the polymer and thus allows it to be handled by the gear-pump and devolatilizer at lower temperatures than if it were pure polymer. Consequently, typical melt temperatures, for example 250° C (PMMA), and thus the likelihood of increased optical loss through degradation of polymer, are avoided until after the devolatilizing process. The reduced viscosity also increases the rate of polymerization by increasing molecular mobility. Thus the occlusion of the active (growing) polymer chain-end is reduced, allowing the reaction to progress more easily, by the addition of further monomer molecules. Walling *et al.* [25] demonstrated that the bulk polymerization rate of styrene is almost linear up to approximately 70% conversion, after which it reduces exponentially as molecular mobility is reduced by the increasing viscosity of the reaction mixture.

The reaction rate is also increased by the phenomenon of autoacceleration [26] which is caused by the exothermic nature of the polymerization itself. At Mitsubishi Rayon it was discovered that there was an optimum viscosity of the reaction mixture required to best harness the effects of autoacceleration; too low and the benefits of the exotherm would be lost through convective heat transfer, too high and the reaction would run away, causing localized boiling of the monomer and consequent inhomogeneities. At a temperature of 140° C, this optimum viscosity is achieved by a concentration of polymer in monomer of 62.4% increasing to 79.6% at 160° C.

The main disadvantage of this process, other than its obvious complexity, is the relatively large amount of polymer-to-metal contact and consequent shearing of the melt. This causes the polymer to degrade and ultimately limits the length of a production run. At the beginning of a run, the passage of monomer and polymer effectively flushes impurities from the apparatus. These impurities consequently contaminate the initial fibre produced. The lowest-loss fibre is produced in mid-run, before the build-up of degradation products has caused quality to decline.

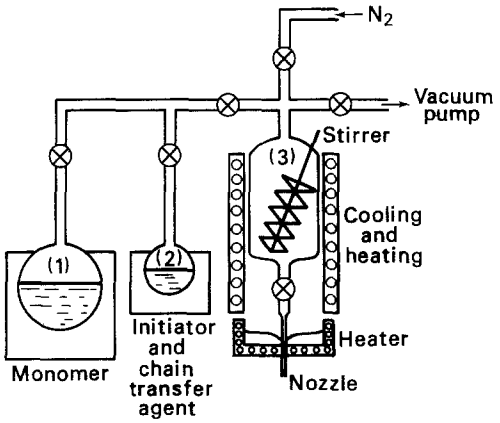

Figure 5 A schematic representation of a batch extrusion process.

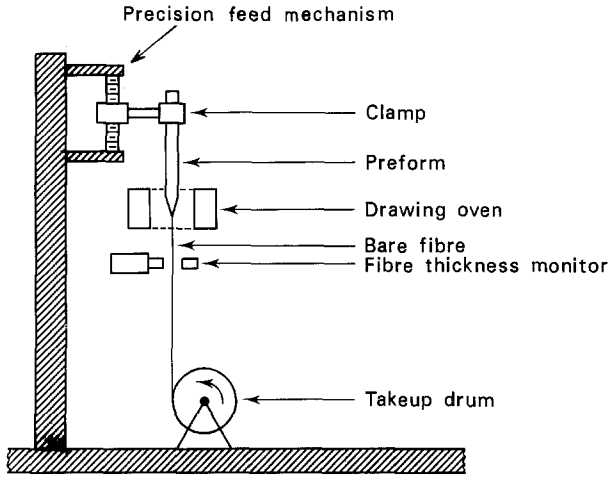

Figure 6 A schematic representation of a preform-drawing process.

3.3. Batch extrusion

A schematic diagram of a batch extrusion process, such as that pioneered by NTT [27], is shown in Fig. 5. The apparatus is evacuated and monomer distilled from the first vessel (1) to the reactor (3) which has been well rinsed with distilled monomer. Chain transfer agent and polymerization initiator are then distilled or sublimed from a second vessel (2) to the reactor (3). The reactor is then sealed and heated at temperatures of up to 180° C to effect polymerization. When 100% conversion of monomer to polymer has been achieved, the temperature is raised to around 200° C and molten polymer forced from the reactor under pressure using dry nitrogen. This core-polymer is then clad immediately using a technique similar to that employed in the previous process.

The chief advantage of this process over that of Mitsubishi is simplicity, both of process control and design and manufacture of the apparatus. The only major process control problem is in ensuring that the temperature of the reaction mixture is sufficiently high, and thus viscosity sufficiently low, during the final stages of polymerization, to prevent localized boiling due to autoacceleration. The relatively simple nature of the apparatus avoids much of the degradation caused by the Mitsubishi system, and thus it has been proved capable of producing lower loss fibres: 55 dB km^{-1} at 567 nm [22, 27] for a PMMA core fibre compared with 125 dB km^{-1} at the same wavelength for Eska Extra [28].

It is however a batch-process and does require that polymerization be carried out to completion, and thus production rates are severely restricted.

3.4. Preform-drawing

Preform-drawing is a technique which closely parallels that used for the production of conventional optical fibres [29]; a schematic diagram of the process is shown in Fig. 6. A cylinder of polymer, or preform, which has been bulk-polymerized in clean conditions [14, 15], is gradually lowered through a tube oven. The tip of the preform melts on its passage through the oven, allowing fibre to be drawn from it. The temperature of the oven hot-zone is determined by both the diameter and rate of feed of the preform, but is regulated so that the preform tip reaches temperatures of between 200 and 250° C. The cladding may either be incorporated in the preform, or be applied on-line as before.

The technique has several distinct advantages, not least that, in a research situation, both expertise and equipment may be carried over from work on conventional fibres. Low losses should be attainable since, like the NTT process, the polymer is subjected neither to prolonged high temperature nor mechanical work, which may induce degradation. However, there are insufficient published data to support this supposition. Ultimately, the chief advantage of preform-drawing may prove to be its versatility. Preforms could be manufactured with complex refractive index profiles which would then be reproduced in the fibre. Thus the process could allow the production of more complex guiding structures than the simple step-index produced by the extrusion-based methods.

Despite its advantages, the technique has not been widely adopted; this is most likely due both to its "batch" nature and the relative lack of development of the POF market. However, it is reported to have been used in the USSR as early as 1968 [30] and it is currently employed by Optectron [31, 32] to manufacture POFs on a commercial scale.

4. Optical properties

The spectral attenuation curves of both a conventional, silica-based fibre [33] and a polystyrene-core fibre, produced at Southampton, are shown in Fig. 7. The optical inferiority of the polymer is immediately apparent, with a minimum attenuation of 187 dB km^{-1} (672 nm) compared with 0.58 dB km^{-1} (1300 nm) for the conventional fibre. However, it is also apparent that the various mechanisms contributing to these losses are similar; it is merely their relative magnitudes and interactions which distinguish the two fibres.

The effects of four separate loss mechanisms are evident in Fig. 7: wavelength-independent scattering, Rayleigh scattering, and absorption in the infrared and ultraviolet regions. Wavelength-independent scattering, which is generally caused by imperfections introduced during the fabrication processes, is negligible in silica-based fibres.

The loss caused by both Rayleigh scattering and the ultraviolet absorption edge decreases with increasing

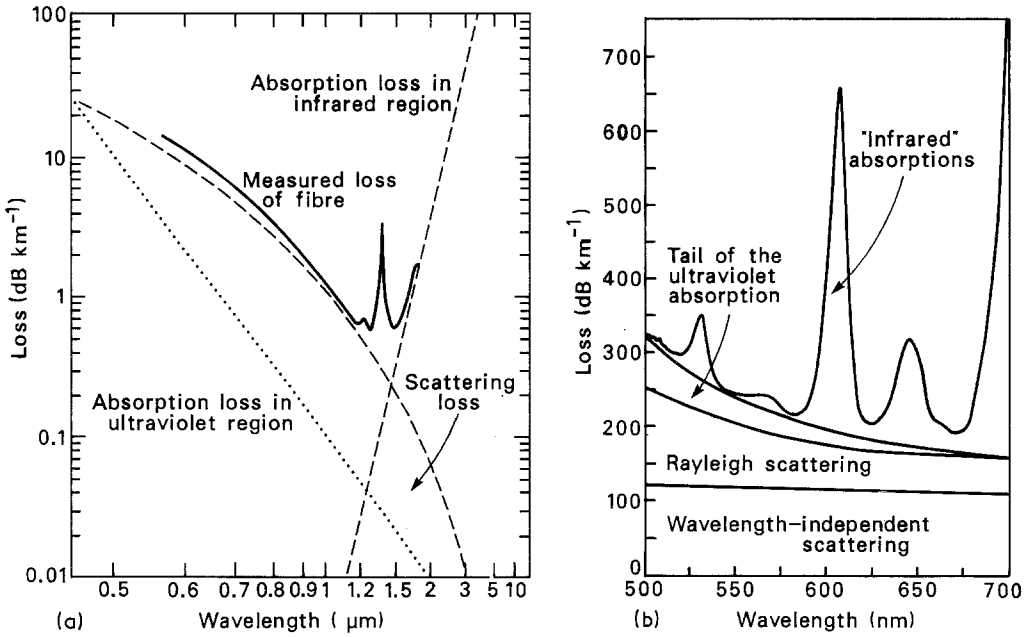

Figure 7 Representative attenuation curves for (a) silica-based and (b) PS-core fibres.

wavelength, whereas the intensity of absorption bands in the infrared increases. Thus, low-loss regions (windows) occur where the combined effect of these mechanisms is minimized. Unfortunately, the molecular structure of polymers causes the "infrared" absorptions to intrude well into the visible region. Consequently, the low-loss windows of polymer fibres occur in relatively narrow bands in the visible, where the effects of Rayleigh scattering and the ultraviolet absorption edge are still substantial.

It should be noted that the attenuation of a POF is determined almost exclusively by the properties of the core material. In a typical POF, the optical field does not penetrate very far into the cladding; it may be shown that for such a fibre, a 3 μm thickness of cladding is sufficient to reduce the ratio of field intensity at the cladding boundary to that in the core at the core-cladding interface [34] to approximately 10^{-12}. Thus, the optical quality of the cladding polymer need not be as high as that of the core material; a fact demonstrated by the production of fluorinated ethylene–propylene co-polymer (FEP) clad silica fibres with an attenuation of 14 dB km^{-1} despite an estimated cladding loss of 5×10^5 dB km^{-1} [35].

4.1. Wavelength-independent scattering

The presence of large inclusions or high-frequency variations in the diameter of the core of the fibre will scatter light, irrespective of wavelength. Here "large" may be taken to mean greater than one micrometre [23] and "inclusions" to encompass particulates, voids and cracks.

The mechanisms responsible for such scattering are illustrated schematically in Fig. 8. Incident light is deviated, mainly by surface reflection; however, refraction, diffraction and even absorption may be involved, depending on the nature of the inclusion. Atmospheric dust provides a ready source of particulates, consequently any system capable of producing low-loss fibres must be scrupulously dust-free.

An NTT patent [27] states that single particles of this kind cause a loss of around 10^{-3} dB m^{-1} and are present in "clean" commercial monomers in concentrations of approximately 100 mm^{-3}. Although this represents a minute volume fraction ($\sim 1.25 \times 10^{-6}$ assuming a 4 μm particle), using a 0.5 mm fibre as an example, the likely loss from particulates is about 2×10^4 dB km^{-1}. Fibres have been produced at Southampton from samples of commercial polymers with minimum attenuations as high as 3×10^4 dB km^{-1}. Losses may be reduced to a few hundred dB km^{-1} simply by employing bulk polymerization and rinsing the apparatus in distilled monomer, in a dust-free environment.

4.2. Rayleigh scattering

Rayleigh scattering is caused by minute irregularities within the propagation medium. The physical size of these irregularities is of the order of one-tenth of a wavelength or less; each irregularity acts as a scattering centre. Although Rayleigh scattering may be caused by fluctuations of both material density and composition, work at NTT has shown that that of PS and PMMA is caused almost entirely by the former. Kaino *et al.* [22] monitored the scattering from samples of styrene and methylmethacrylate as they polymerized. Despite the apparent gross compositional variations of the monomer–polymer mixture,

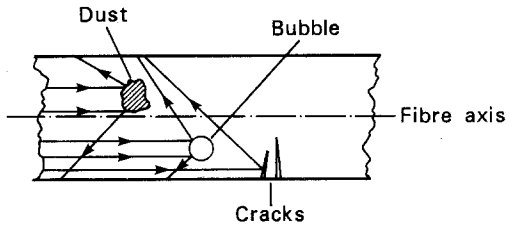

Figure 8 A schematic representation of mechanisms responsible for wavelength-independent scattering.

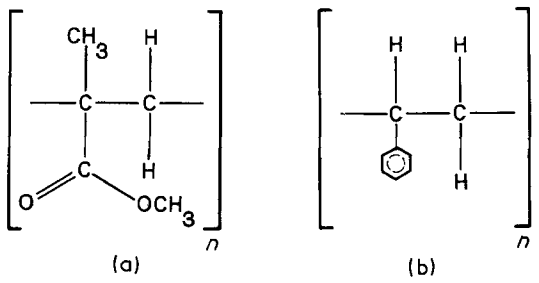

Figure 9 The molecular structures of (a) PMMA and (b) PS.

scattering intensity reached a constant value at around 70% conversion in both cases.

Since an amorphous material, by definition, maintains its liquid structure as it solidifies from the melt, all such materials may be treated as supercooled liquids. Thus the turbidity (τ) of an amorphous polymer (representing the variation of scattering intensity with wavelength) may be calculated from the following equation [36]:

$$\tau_{(ISO)} = \frac{8\pi^3}{3\lambda^4}\left[\varrho\left(\frac{\partial\varepsilon}{\partial\varrho}\right)_T\right]^2 kT_f\beta_T \quad (2)$$

In this equation it is assumed that the scattering, caused by minute density fluctuations, may be accurately modelled as that due to a regular arrangement of discrete, spherical particles. The fictive temperature (T_f) is the glass transition temperature, below which the "scattering structure" is frozen in.

Owing to the difficulty in obtaining reliable values of $(\partial\varepsilon/\partial\varrho)_T$ directly, it is normally determined from empirical expressions, such as the Clausius–Mossotti equation [36]:

$$\varrho\left(\frac{\partial\varepsilon}{\partial\varrho}\right)_T = \frac{(n^2 - 1)(n^2 + 2)}{3} \quad (3)$$

Hence Equation 1 becomes

$$\tau_{(ISO)} = \frac{8\pi^3}{3\lambda^4}\left(\frac{(n^2 - 1)(n^2 + 2)}{3}\right)^2 kT_f\beta_T \quad (4)$$

In reality, this isotropic model is too simple. The scattering from a polymer composed of long, branched or even crosslinked chains may often be better modelled as that due to a regular arrangement of ellipsoidal particles. The result is that a correction factor must be applied to increase the value of turbidity given by Equation 4. This correction is known as the Cabannes factor [37] and is given by

$$C_u(90) = \frac{6 + 6\varrho_u(90)}{6 - 7\varrho_u(90)} \quad (5)$$

The Rayleigh scattering loss of PMMA is significantly lower than that of PS; this may be explained with reference to their molecules (represented in Fig. 9) and Equations 4 and 5. The presence of the benzene ring in PS has two detrimental effects. Firstly, it serves to raise the refractive index of the material (1.59) above that of PMMA (1.49) and thus increase turbidity, as may be deduced from Equation 4. Secondly, the flat physical geometry of the ring increases molecular anisotropy and hence scattering; by comparison, the tetrahedral methyl group (CH_3) in PMMA creates a far more three-dimensional structure. The result is that the value of the Cabannes factor correction for molecular anisotropy, given by Equation 5, is about 2.7 for PS [38] yet only 1.1 for PMMA [39]. The corresponding values of turbidity at 633 nm are 55 dB km^{-1} (PS) and 13 dB km^{-1} (PMMA) [22].

4.3. Quasi-extrinsic wavelength-dependent scattering

Although polymer glasses such as PS and PMMA may generally be described as amorphous, the complex chain-like nature of the polymer molecule allows the formation of partial alignments and other substructure. Such alignments are well known and have been suggested as a cause of increased scattering intensity in glassy PMMA [39, 40]. In addition, further inhomogeneities, resulting from strain-induced birefringence [38], may be created during the fibre-forming process, due to the high photoelastic coefficients of the materials [41].

Being quasi-extrinsic, the effects of such mechanisms on loss are impossible to quantify. However, it is likely that the variation of loss with wavelength will have a similar form to that of Equation 4. That is:

$$\tau = A\lambda^{-n} \quad (6)$$

where n may be between zero and four, as the effective size of the inhomogeneities, relative to the wavelength of the light decreases [23].

4.4. Ultraviolet band-edge absorption

Polymers, in common with all solids, absorb light in the ultraviolet region of the spectrum. The mechanism responsible for this absorption depends on transitions between electronic energy levels of the bonds within the materials; the absorption of a photon causes an upward transition, leading to an excitation of the electronic state of the solid.

In PMMA, the most significant absorption is caused by the transition of the n-orbital to a π^* orbital of the double bond within the ester group of the molecule. Again, it is the benzene ring which increases the loss of PS; the π to π^* transitions within the delocalized bonds of the ring produce an extremely intense absorption.

Other compounds employed in polymer synthesis, such as initiators and chain-transfer agents, give rise to similar absorptions of their own. Examples [22] of these absorptions are shown in Fig. 10. In this case the initiator used was azo-t-butan. As a result of the NTT work [27] azo-compounds are used in preference to organic peroxides because of their less intense ultraviolet absorption.

The original work by Urbach [42] and later experimentation in fibres by Pinnow *et al.* [43] show that ultraviolet absorption decreases exponentially with wavelength. Consequently, due to the relatively short wavelengths at which low-loss windows are located in polymers, the contribution to the total, minimum attenuation of a fibre is significant.

The relationships between wavelength and absorption have been determined empirically for both PMMA and PS by Kaino and co-workers and are

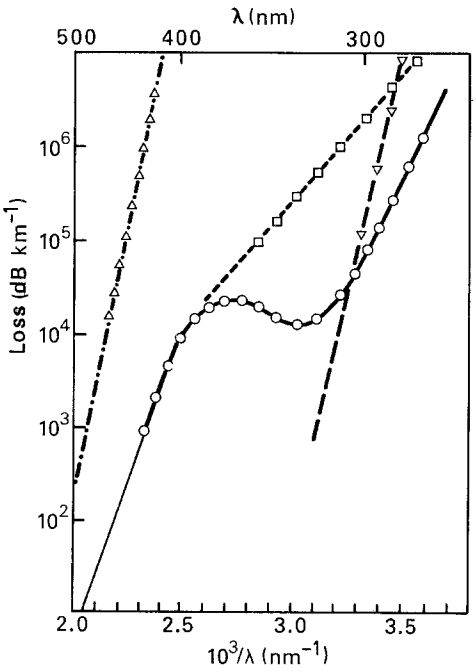

Figure 10 The ultraviolet absorption of (○) PMMA and its raw materials: (△) azo-t-butan, (□) n-BuSH, (▽) MMA.

given in Equations 7 [22] and 8 [18]:

$$\alpha_e\,(\text{PMMA}) = 1.58 \times 10^{-12} \exp\left(\frac{1.15 \times 10^4}{\lambda}\right) \quad (7)$$

$$\alpha_e\,(\text{PS}) = 1.10 \times 10^{-5} \exp\left(\frac{8.0 \times 10^3}{\lambda}\right) \quad (8)$$

From these equations it may be determined that the attenuation due to the ultraviolet band-edge absorption in PS is around 100 dB km^{-1} at 500 nm and 7 dB km^{-1} at 600 nm, whereas in PMMA it is below 1 dB km^{-1} above 500 nm.

4.5. Contamination due to transition metal ion contamination

Absorption may also be caused by electronic transitions within contaminants. The phenomenon of loss caused by the presence of transition metal ions in silica-based fibres has been well documented [44]. Since the characteristic absorptions of ions of materials such as iron, manganese and cobalt are centred in the visible spectrum, a parallel mechanism in polymers would be catastrophic. Consequently, the need to reduce transition metal ion contamination to the parts per billion level is stressed in all POF patents. However, to date, no absorptions observed in the POFs examined at Southampton (which have included both low-loss commercial fibres and those drawn from polymer rods, not intended for optical use) have been positively identified as being caused by transition metal contaminants. This is most likely due to a combination of the low solubility in monomers and the low vapour pressures of transition metal salts. The latter allows purification of the monomers by distillation, in the same manner as the dopant-liquids used in silica-based fibre manufacture [45, 46].

4.6. Infrared vibrational absorption

The attenuation curve of a PS-core fibre is shown in Fig. 7a and that of a PMMA-core fibre in Fig. 11. In both cases the absorption bands are caused by the 5th, 6th and 7th harmonics of the stretching vibrations of the carbon–hydrogen bonds in the materials (designated ν_5 to ν_7), with smaller contributions from their stretching and bending vibrations (designated $\nu + \delta$). The fundamental frequency of the stretching vibrations of the carbon–hydrogen atom-pair may be calculated from the equation [47]

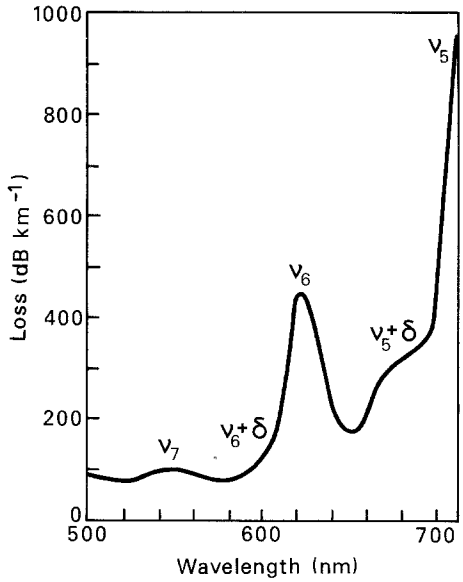

Figure 11 The attenuation curve of a PMMA-core fibre.

$$\nu_0 = \left(\frac{K}{4\pi^2\mu}\right)^{1/2} \quad (9)$$

where μ is the reduced mass of the system, defined as

$$\mu = \frac{m_1 m_2}{m_1 + m_2} \quad (10)$$

Since the vibration is not truly harmonic, additional absorptions (or harmonics) occur at approximate multiples of the fundamental frequency. The intensities of such absorptions decrease by one order of magnitude with each harmonic, illustrated for the case of PMMA in Fig. 12 [22].

Hydrogen, being the lightest of atoms, causes the

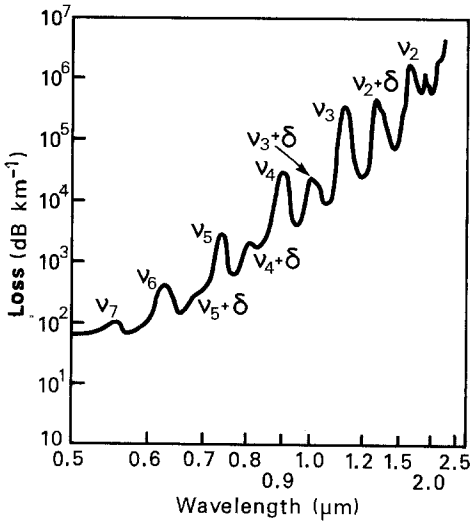

Figure 12 The infrared absorption of PMMA.

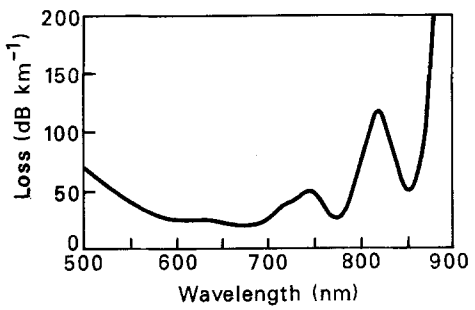

Figure 13 The attenuation curve of a PMMA-D8-core fibre.

fundamental of the C–H vibration to occur at the relatively short wavelength of 3.2 μm (in PMMA), and thus the high harmonics intrude upon the visible spectrum.

4.7. The modification of absorption spectra by atomic substitution

It is clear from Equations 9 and 10 that if the reduced mass of the atom-pair were increased, by replacing hydrogen with a more massive atom, the wavelengths of the fundamental vibration and subsequent harmonics would also be increased. Thus, the low-loss windows of a POF made from such a material would move to longer wavelengths, where losses due to both Rayleigh scattering and the ultraviolet absorption edge are reduced.

This approach was first suggested by Schleinitz [13] who demonstrated that, by employing a fully deuterated PMMA (PMMA-D8) as a core material, the wavelengths of the low-loss windows could be increased and attenuation reduced. The technique was later refined by Kaino *et al.* [21], who succeeded in producing a PMMA-D8 core fibre with a minimum attenuation of 20 dB km^{-1} at 680 nm. The attenuation curve of this fibre is shown in Fig. 13. The fundamental vibration of the carbon–deuterium bond occurs at approximately 4.4 μm, compared with 3.2 μm for carbon–hydrogen, resulting in an upward shift of 200 nm for the seventh harmonic.

4.8. The loss limits of PS- and PMMA-core polymer fibres

The contributions to total loss of the various loss mechanisms, and consequent theoretical limits, of both PS-core and PMMA-core fibres are catalogued in Tables I and II [22].

It is apparent from these tables that although PMMA may exhibit the lower loss, polystyrene displays a distinct advantage at longer wavelengths. This is because the vibrational absorptions of the methyl and methylene groups in PMMA overlap to give a broad, intense peak, whereas those of the aliphatic and aromatic absorptions in PS are quite separate. Thus, the aromatic and aliphatic absorption bands, with their respective narrow linewidths and low intensities, have less influence on the low-loss windows of PS than the methyl and methylene absorption bands on those of PMMA.

TABLE I Loss mechanisms and limits for a PMMA-core POF

Loss mechanism	Wavelength (nm)		
	518	567	650
Vibrational absorption	1	7	88
Rayleigh scatter	28	20	12
Loss limit (dB km^{-1})	29	27	100

TABLE II Loss mechanisms and limits for a PS-core POF

Loss mechanism	Wavelength (nm)			
	552	580	624	672
Vibrational absorption	0	4	22	24
Band-edge absorption	22	11	4	2
Rayleigh scatter	95	78	58	43
Loss limit (dB km^{-1})	117	93	84	69

Optical sources have yet to be tailored to polymer requirements, and thus those supplied for use with commercial PMMA-core POFs would typically be GaAsP LEDs emitting at 665 nm. Consequently, the practical loss limit of a PS-core fibre is currently lower than that of a PMMA-core fibre. However, commercial fibres are almost exclusively based on PMMA because of its vastly superior mechanical properties.

Interest in deuterated polymers is limited due to the prohibitive materials costs.

5. The present market penetration and future developments

Major application areas which are immediately apparent include data-systems in both automobiles and aircraft, LANs, and related sub-groups such as inter- and intra-office networks. There is also speculation that, with the growing importance of computing and video, intra-home systems may soon be required; these too could provide a good market for POFs.

The performance of the current market leader Mitsubishi Eska Extra is outlined in Table III. Unfortunately, most of the suggested applications require significantly higher performance than is represented by such figures. Consequently, the uses to which fibres have been put have not taxed their capabilities. For example, the lengths of fibre used in typical applications, such as headlamp monitors in automobiles, "pigtails" for optical sensors and links between computer keyboards and processing units, are often less than 5 m. The 3500 dB km^{-1} fibres described in the initial Mitsubishi patent would have been capable of transmission over such distances; the 200 dB km^{-1} or so available from commercial fibres is rarely required.

5.1. Low-loss POFs

The low overall cable cost of POFs would appear to make them suitable for use in relatively short distance, high connector-density systems such as LANs. In turn, the market is extremely attractive offering the

TABLE III The performance of Eska Extra

Attenuation (567 nm)	Attenuation at source wavelength (665 nm)	Maximum continuous operating temperature	Bandwidth
125 dB km^{-1}	220 dB km^{-1}	80° C	2.5 MHz km

prospect of a high and continuously expanding volume of sales. Unfortunately, the attenuation of commercially available fibres is too high.

Assuming a maximum transmission length of 500 m and a system budget of 30 dB with a 5 dB margin (to allow for connectors) a target attenuation of 50 dB km^{-1} results. It is clear from Table I that such a figure is well within the loss limits of PMMA with 29 and 27 dB km^{-1} possible at 518 and 567 nm, respectively. Moreover, NTT have achieved 55 dB km^{-1} under laboratory conditions and Asahi Chemical Co. have recently announced its Luminous™ POF with a claimed 65 dB km^{-1} at 567 nm [48]. Thus, it seems likely that the required 50 dB km^{-1} will be achieved using conventional PMMA by further improvements in fabrication techniques and the consequent reductions in extrinsic losses.

In the event of PMMA-core POFs being accepted as transmission media for LANs, the position of the low-loss window of the material is unlikely to remain a problem; the development of sources capable of operating at the 567 nm primary window will almost certainly be stimulated by the prospect of extremely high-volume sales.

The effects of deuteration have already been discussed. It is feasible that heavier atoms, in particular fluorine and chlorine, may be employed in similar substitutions, to similar effect. If all the carbon–hydrogen atom-pairs within a polymer were substituted for carbon–fluorine, or carbon–chlorine, the resulting increases in reduced mass would cause the fundamental absorptions to shift to approximately 8 and 13 μm, respectively [49]. This shift would allow access to even longer wavelengths, and thus lower-loss transmission windows than is possible with deuteration.

Unfortunately, the optical properties of the available perhalogenated polymers make them unattractive for POF use. Not only do materials such as poly(tetrafluoroethylene) (PTFE) and poly(chlorotrifluoroethylene) (CTFE) exhibit high degrees of crystallinity [50], but their monomers are also unsuitable for bulk polymerization. Thus, substantial losses arise from both intrinsic and extrinsic wavelength-independent scattering.

The potential of even crystalline halogenated polymers as optical elements was noted by the Western Electric Co., who filed a patent in 1973 to cover their use in such applications [51]. Here, the problems associated with crystallinity were circumvented by quenching the molten polymer at rates of around 100° C sec^{-1}. Thus, the amorphous state of the melt could be "frozen in" before any crystal-forming molecular alignments had time to occur [52].

Although the degree of transparency achieved by quenching may be adequate for, for example, a lens, problems would be likely to arise if the technique were applied to a POF. The depth of penetration of the quench may not be great enough to eliminate crystallinity throughout the entire fibre. In addition, any fibre so treated would be liable to recrystallize as the result of temperature cycling experienced in service.

Crystallinity may also be reduced by the presence of bulky atoms or molecules as side-groups to the polymer chains. These side-groups disrupt molecular packing and thus reduce their ability to form alignments; for example, the presence of the bulky chlorine atom in CTFE causes it to exhibit reduced crystallinity compared with PTFE. Since this mechanism is both wholly intrinsic and irreversible it is preferable to quenching.

If a totally amorphous, perhalogenated polymer could be engineered, its potential as a low-loss material for POFs would ensure keen interest; in this event, the problems of cleanliness associated with non-bulk polymerization are unlikely to prove insurmountable.

The difficulties encountered in the synthesis of perhalogenated polymers of sufficient optical quality for POFs have led to the investigation of partially halogenated materials. In particular, attention has been focused on fluorinated analogues of PMMA. It is hoped that these materials may ultimately provide the best compromise, combining amorphous nature and bulk-polymerizability with low infrared absorption, through reduced hydrogen content and low Rayleigh scattering from the reduced refractive index.

However, the residual hydrogen atoms in such materials still give rise to their characteristic absorption bands. Although the intensities of these bands will be reduced, their influence in the near-infrared may still be sufficiently strong to interfere with the low-loss windows accessible in a perfluorinated polymer.

Thus, the reduction in attenuation is achieved through the reduced intensities of the residual carbon–hydrogen vibrations, rather than the shift of absorptions to longer wavelengths caused by fluorine substitution. In addition, although the reduction in refractive index caused by the presence of the fluorine also reduces Rayleigh scattering (as may be deduced from Equation 3) in a practical situation, reduction of attenuation by this method is tempered by the need to find a cladding material of still lower index. Thus, reductions in attenuation from partial halogenation are likely to be small, of the order of a few dB km^{-1} rather than tens of dB km^{-1}.

The effects of reducing the hydrogen content of acrylic monomers were investigated by Boutevin *et al.* [53]. Their results are shown in Fig. 14 and clearly indicate the reduction in absorption intensity; a similar reduction may be expected in the corresponding polymers.

Researchers at ICI have reported work on methacrylate-type polymers, of the form shown in Fig. 15 [51], which show promise as low-loss POF materials; R1 and R2 represent halogenated groups. The refractive indices of fluorinated forms of these materials can be as low as 1.32, making cladding virtually impossible. However, higher indices may be obtained by employing chlorine substitutions, although at the expense of temperature stability.

The question of the ultimate loss-limit of POFs, employing polymers which can be synthesized using well-tried, clean techniques, was addressed by Kaino

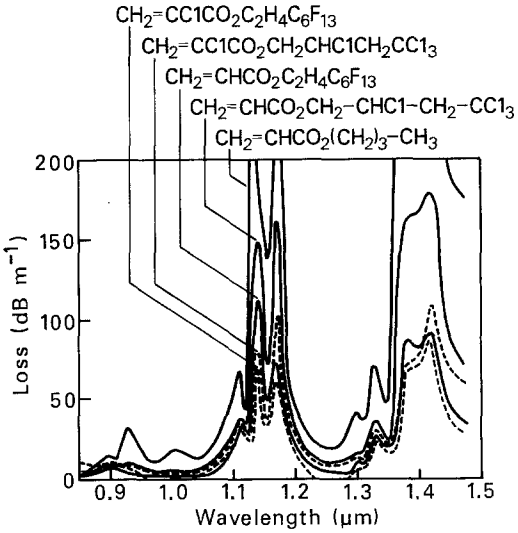

Figure 14 The infrared absorption of fluorinated acrylic monomers.

[54]. He suggested the use of poly(hexafluorobutylmethacrylate) as a core-material for which a loss-limit of 19 dB km^{-1} at 567 nm was estimated. Substitution of the remaining hydrogen atoms with deuterium resulted in a predicted loss of 5 to 6 dB km^{-1} at 680 nm as against 9 to 10 dB km^{-1} for deuterated PMMA. The reduction in loss over that of PMMA, which may be attributed to partial fluorination, is caused by reduced Rayleigh scattering. This reduction results from the extremely low refractive index of the material. Unfortunately, at 1.32, the index is too low for known polymers to be used as cladding. Thus the practical loss-limit, allowing for some reduction in index through fluorination, must lie between 5 and 10 dB km^{-1}.

5.2. High-bandwidth POFs

The attenuation of POFs is being reduced to the extent that they may soon be considered as viable data-transmission media for systems such as LANs and intra-office networks. Consequently, the data-carrying capacity, or bandwidth, of POFs has become of increased importance.

Information transmitted through an optical fibre is coded as a series of pulses of light, or "bits". Each pulse is made up from a great many rays, with each ray entering the fibre at a different angle of incidence, θ. The range θ depends on the NA of the fibre. This situation is represented for a step-index fibre in Fig. 16a. The path-length of each ray is different so that the pulse spreads as it travels along the fibre. After the pulses have travelled a certain distance, this spreading causes them to overlap to such an extent that the information which they contain becomes scrambled. Thus, the bandwidth of the fibre is limited.

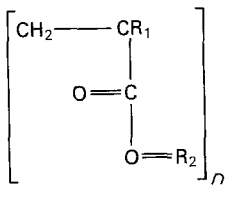

Figure 15 The general structure of the halogenated polymers investigated by ICI.

The extent of pulse-spreading may be estimated by calculating the delay-time (δt_s) between an axial ray and an extreme meridional ray of a pulse [55]. The extreme meridional ray is that at the limit of the fibre NA. These rays are designated A and M, respectively, in Fig. 16a. It may be shown that:

$$\delta t_s \simeq \frac{(\mathrm{NA})^2}{2n_1 c} \tag{10}$$

Assuming there is no overlap between pulses, the maximum bit-rate $\beta_T(\max)$ of the fibre is therefore:

$$\beta_T(\max) \simeq \frac{1}{2\delta t_s} \tag{11}$$

$\beta_T(\max)$ is equal to the bandwidth of the fibre expressed in Hertz. Since bandwidth is inversely proportional to distance, the bandwidth–length product (Hz km) is normally adopted as a more useful parameter of the information-carrying capacity of a fibre.

Applying Equations 11 and 12 to the case of a POF, for example Mitsubishi Eska (NA = 0.5, n_1 = 1.49), a bandwidth–length product of 1.8 MHz km results. A more sophisticated analysis, which allows for some overlap between pulses, produces a closer estimate of 2.5 MHz km. Unfortunately this is inadequate to cope with much of the proposed traffic over the 500 m distances envisaged in low-loss applications; analogue video signals require 6 MHz km, high-resolution graphics 10 MHz km and digital video 40 MHz km [56].

It may be seen from Equation 11 that bandwidth can be increased by reducing NA. A reduction in the NA of Eska from 0.5 to 0.25 would increase its bandwidth to around 10 MHz km, but at the expense of lower launched power.

A technique which is widely used to increase the bandwidth of silica-based fibres involves grading the index of the core to produce a profile which approximates to a parabola [57]. Thus, axial rays travel in higher-index material and therefore more slowly than meridional rays, which now follow curved paths within the lens-like structure formed by the index gradient. The overall effect is to reduce the difference in transit times (δt_s) between the rays which make up a pulse and thus increase the bandwidth. This situation is represented in Fig. 16b.

Graded-index POFs may be fabricated by preform-drawing techniques. Two methods for the production of preforms with the required refractive index profile have been reported by Ohtsuka and co-workers; two-step co-polymerizations [58, 59] and photo-co-polymerization [60–64]. The former involves the immersion of a partially polymerized rod in a co-monomer of lower refractive index. This co-monomer diffuses into the rod and sets up the refractive index gradient which is "fixed" by further polymerization. The main monomers used have been diethylene glycol bis(allylcarbonate) (CR-39) for the pre-polymer rod, and fluorinated methacrylates. The CR-39 polymers produced have been predominantly cross-linked. This cross-linking is advantageous in that it allows the

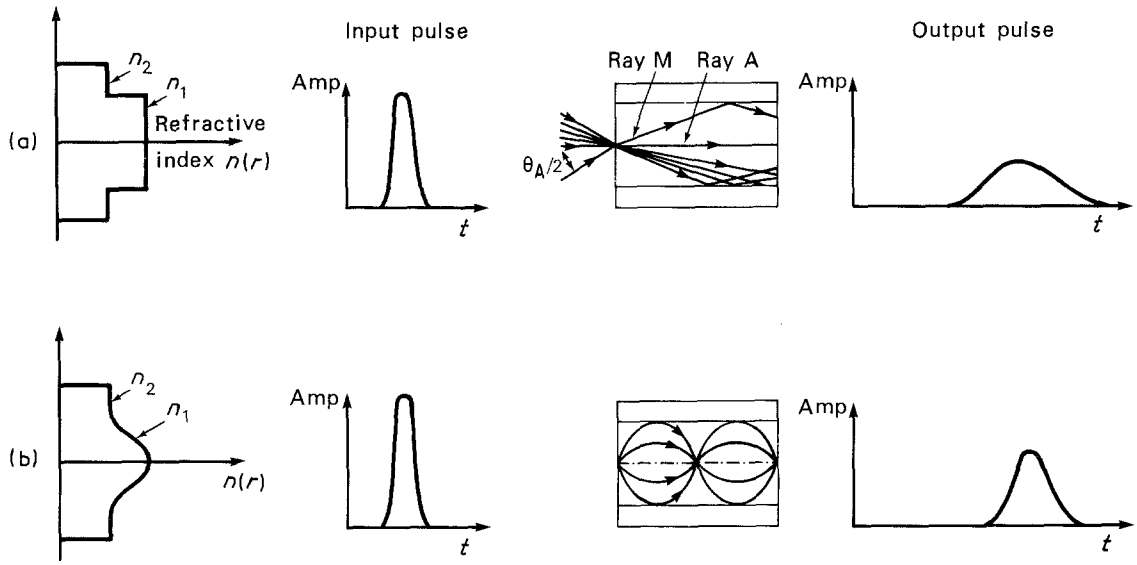

Figure 16 Schematic diagrams showing (a) a multimode step-index fibre and (b) a multimode graded-index fibre, and illustrating the pulse-broadening in both fibre types.

co-monomer to penetrate the pre-polymer rod, without dissolving it too extensively. However, the intermolecular bonds within a cross-linked material prevent it from flowing under the action of heat. Thus, the resulting preforms could not be melt-processed into POF.

The second method has been used to produce preforms of linear co-polymers which could then be drawn into POFs. In this process two monomers, of different refractive indices and containing an ultraviolet-sensitive initiator, are sealed in a glass tube. This tube is then rotated about its vertical axis and illuminated externally by ultraviolet light. A zoned polymerization is effected by means of a mask which traverses the outside of the tube. A schematic representation of the process is shown in Fig. 17 [60]. The monomers are chosen such that their reactivity ratios cause the lower refractive index material to polymerize preferentially near the outside of the tube during the early part of the reaction. Varying degrees of co-polymerization then take place until the polymerization is dominated by the second monomer during the latter stages of the reaction, towards the centre of the preform.

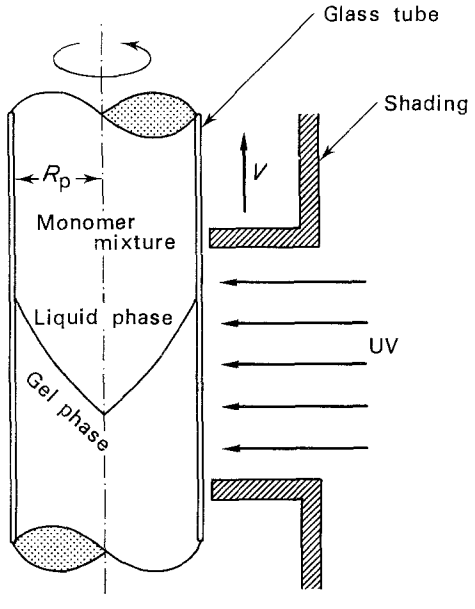

Figure 17 A schematic representation of the photo-co-polymerization process.

It was found that in a binary co-polymer system the refractive index profile achieved deviated significantly from that desired, particularly around the centre of the preform. By utilizing a third co-monomer of high refractive index, a closer approximation to the ideal could be obtained. However, this enhancement further complicates the choice of monomers; the solubility parameters of the three homopolymers must be approximately equal to ensure that no phase-separation takes place and a transparent polymer results [64]. The two systems which appear most promising are methyl methacrylate–acrylonitrile–vinyl benzoate and methyl methacrylate–benzyl acetate–vinyl benzoate.

These preforms and fibres have been investigated principally for their light-focusing and image-guiding properties. Losses reported have been very high, with a minimum of 1070 dB km^{-1} at 670 nm for a fibre of methyl methacrylate–vinyl phenylacetate co-polymer [62]. Consequently, no claims have been made of increased bandwidth over simple, step-index POFs. However, most of this loss was attributed to extrinsic scattering and thus significant improvements may be expected from refinements to fabrication techniques. Thus, in theory, the production of a low-loss, high-bandwidth POF is possible.

5.3. High-temperature POFs

Data transmission systems in both automotive and aerospace applications provide further large potential markets for POFs. The distances involved in such systems are much shorter than those in LANs, and consequently the loss requirements are far less stringent; assuming maximum fibre runs of 10 m for automotive and 50 m for aerospace use, losses of 1000 and 200 dB km^{-1}, respectively, should be adequate.

Unfortunately, the present temperature ceiling for POFs of around 80° C is too low. Underbonnet

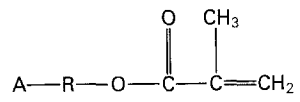

Figure 18 The general structure of the high carbon-number alkyl methacrylates.

applications in automobiles require performance at 125° C for 1000 h and it is possible that other areas, for example behind the dashboard, may reach temperatures above the current 80° C ceiling. Aerospace environments are even more severe and consequently demand performance at temperatures in excess of 140° C.

Although it may be possible to protect fibres from short-term exposure to high temperatures by means of an insulating jacket, applications involving longer-term exposure will require the development of high-temperature polymers for use as core-materials. The high-temperature performance of a polymer is limited by its glass transition. For both PS and PMMA, T_g lies between 100 and 105° C. However, in practice, the presence of up to 1% free monomer has a plasticizing effect which may reduce this figure to as low as 90° C [65]. At temperatures above T_g both mechanical and optical performance decline.

The form of Equation 3 indicates that Rayleigh scattering will increase with increasing temperature. However, since the "scattering structure" of the material is frozen at T_g, the change below this temperature is negligible. Although this increase in scattering is reversible if the polymer is maintained at high temperature for extended periods, oxidation may cause irreversible optical loss through a broadening of the ultraviolet edge.

Mechanical problems arise from both the softening of the material and the relaxation of molecular alignment which result from the action of heat. The latter is irreversible and thus will reduce the mechanical performance of the material when cooled. In addition, the accompanying contraction may cause fibres to migrate out of connectors and other devices.

Thus, materials with glass transition temperatures above those of PMMA and PS are required to increase the temperature ceiling of POFs. The T_g of polycarbonate is around 170° C. Although it may not be bulk-polymerized and thus exhibits high extrinsic scattering losses, there have been several reports from Japan of high-temperature fibres based on this material. Quoted losses have been of the order of 1000 dB km^{-1}, which would be adequate for automotive use.

Polymers of the high carbon-number alkyl methacrylates both have higher T_gs than either PMMA or PS and may be bulk-polymerized. These materials have the general form shown in Fig. 18, where A represents an alicyclic hydrocarbon group and R an alkyl group. Their use as materials for POFs was proposed by the Sumitomo Chemical Co. [66], placing particular emphasis on co-polymers and terpolymers of bornyl, menthyl, fenchyl and adamantyl methacrylates with methyl methacrylate.

Using various copolymers of vinylidene fluoride as cladding materials, the optical performance of several of these polymers was assessed at temperatures of up to 150° C. Many showed increases in attenuation of around 20 dB km^{-1} at temperatures as low as 70° C, rising to around 150 dB km^{-1} at the higher temperatures. However, in all cases their performance was superior to that of PMMA-core fibres, produced using the same process. These fibres exhibited increases of 150 dB km^{-1} at 70° C, rising to over 1000 dB km^{-1} after 7 h at 105° C. The best performance was achieved using a 15:83:2 terpolymer of bornyl methacrylate, methyl methacrylate and methyl acrylate, which showed no increase in loss even after 6 h at 125° C.

The quoted minimum losses of these fibres, including those with cores of PMMA homopolymer, were between 350 and 500 dB km^{-1} at room temperature. These relatively high values give no indication of either the absolute limits or the comparative magnitudes of the losses of such polymers, since production conditions were standardized throughout the tests rather than optimized for each material. It is possible that the small increases in attenuation witnessed at temperatures significantly below T_g were caused by production-related mechanisms. For example, wavelength-independent scattering could have been increased by disruption of the core-clad interface, caused by an expansion mismatch between the two materials.

The fluorinated alkyl methacrylate polymers investigated by ICI (Fig. 15) also show promise as high-temperature materials, although they remain untried in fibre form. T_gs in excess of 160° C have been reported for such polymers in which R_2 is a fluorinated ring [50]. However, the presence of this ring dictates that high T_g and very low loss are unlikely to coincide in materials of this type.

The increase in refractive index induced by the ring is, on balance, advantageous; it facilitates cladding at the expense of increased Rayleigh scattering. On the other hand, further increases in loss are likely to result from the effects of greater molecular anisotropy (c.f. Equation 4) and enhanced ultraviolet edge; together, these effects would almost certainly outweigh those of reduced vibrational absorption. However, the molecular structures of these polymers give no indication that their optical performance should be any worse than that of conventional aromatic materials such as PS. Thus, it is likely to be good enough for any envisaged high-temperature application.

There is no doubt that the use of high-T_g polymers would greatly improve high-temperature performance. However, care must be taken in their synthesis to preserve the elasticity essential to POFs. The relationship between T_g and elasticity in a polymer is highly complex. It is influenced not only by molecular weight and molecular weight distribution but also by mechanisms such as crazing and orientation-hardening. However, at room temperature the elastic limit of a low-T_g polymer is likely to be greater than that of a high-T_g polymer. This statement is supported by the Sumitomo work which revealed that, despite pre-orientation, 0.8 mm diameter fibres of high-T_g polymers could fracture at bend radii as high as 10 mm. As in other applications, the utility of high-temperature

POFs is dependent on their flexibility being significantly greater than that of silica-based fibres.

Although several Japanese companies, including Mitsubishi Rayon and Fujitsu, have either announced the imminent launch of high-temperature POFs or actually include them in their product list, they are not yet generally available outside Japan.

6. Conclusion

The potential advantages of POFs as short-range data-transmission media, which derive from their great flexibility and high NAs, have been known for some years. Unfortunately, poor performance in the areas of attenuation, bandwidth and heat-resistance has limited their penetration in important market-segments such as LANs and automobile and aerospace data-systems. However, developments continue which show that such shortcomings are far from insurmountable and point the way to a new generation of high-performance POFs. There can be little doubt that the increased market acceptance which these fibres will warrant will stimulate further progress, both in fibre and allied systems technologies, and thus enable POFs to realise their latent potential.

References

1. A. A. GRIFFITH, *Phil. Trans. R. Soc.* **221A** (1920) 160.
2. H. MURATA, ECOC 12 Barcelona, Spain, Sept. 22–25 (1986) Paper ThA2.
3. R. N. HAWARD, "The Physics of Glassy Polymers" (Applied Science, London, 1973) Ch. 5.
4. G. REHAGE and G. GOLDBACH, *Angew. Macromol. Chem.* **1** (1967) 125.
5. R. N. HAWARD, B. M. MURPHY and E. F. T. WHITE, in Proceedings of International Conference on Fracture, Brighton, 1969, Paper 45.
6. *Idem, J. Polym. Sci. A-2* **9** (1971) 801.
7. D. S. MATSUMOTO and M. T. TAKEMORI, *J. Mater. Sci.* **20** (1985) 873.
8. G. A. BERNIER and R. P. KAMBOUR, *Macromolecules* **1** (1968) 393.
9. R. P. KAMBOUR, *J. Polym. Sci. A* Vol. 2 (1964) 4159.
10. M. R. KAMAL, V. TAN and M. RYAN, in Proceedings of International Conference on Polymer Processing, Massachusetts Institute of Technology, August 1977, edited by Nam P. Suh and Nak-Ho Sung (MIT Press, London, 1977) p. 34.
11. MITSUBISHI RAYON Co., U.K. Patent 1 431 157 (1974).
12. *Idem*, U.K. Patent 1 449 950 (1974).
13. H. M. SCHLEINITZ, in Proceedings of International Wire and Cable Symposium, 1977, Paper 25, p. 352.
14. du PONT de NEMOURS & Co., UK Patent GB 2 006 790 B (1978).
15. *Idem*, UK Patent GB 2 007 870 B (1978).
16. T. C. HAGER, R. G. BROWN and B. N. DERICK, *Trans. Soc. Automotive Eng.* **76** (1976) 581.
17. S. OIKAWA, M. FUJIKI and Y. KATAYAMA, *Elect. Lett.* **15** (1979) 829.
18. T. KAINO, M. FUJIKI and S. NARA, *J. Appl. Phys.* **52** (1981) 7061.
19. T. KAINO, M. FUJIKI, S. NARA and S. OIKAWA, *Appl. Opt.* **20** (1981) 2886.
20. T. KAINO, K. JINGUJI and S. NARA, *Appl. Phys. Lett.* **41** (1982) 802.
21. *Idem, ibid.* **42** (1983) 567.
22. T. KAINO, M. FUJIKI and K. JINGUJI, *Rev. Elect. Comm. Lab.* **32** (1984) 478.
23. S. F. CARTER, P. W. FRANCE, M. W. MOORE and J. R. WILLIAMS, *Mater. Sci. Forum* **5** (1985) 397.
24. P. J. FLORY, "Principles of Polymer Chemistry" (Cornell University Press, New York, 1967) Ch. 5.
25. C. WALLING, E. R. BRIGGS and F. R. MAYO, *J. Amer. Chem. Soc.* **68** (1946) 1145.
26. P. J. FLORY, "Principles of Polymer Chemistry" (Cornell University Press, New York, 1967) Ch. 4.
27. NIPPON TELEGRAPH & TELEPHONE, UK Patent GB 2 089 352 B (1981).
28. MITSUBISHI RAYON Co., Technical Bulletin on Eska Cables.
29. J. E. MIDWINDER, "Optical Fibres for Transmission" (Chapman & Hall, London, 1983) Ch. 9.
30. V. S. CHAGULOV, *Kvantovaya Electron* **9** (1982) 1587.
31. L. R. ALLEMAND, J. CALVET, J. C. CAVAN and J. C. THEVENIN, *Nucl. Instr. Meth.* **225** (1984) 522.
32. C. VINCENT, *Sciences et Techn.* **7** (1984) 17.
33. M. HORIGUCHI, *Elect. Lett.* **12** (1976) 310.
34. A. W. SNYDER and J. D. LOVE, "Optical Waveguide Theory" (Chapman & Hall, London, 1983).
35. P. KAISER, A. C. HART and BLYLER, *Appl. Opt.* **14** (1975) 156.
36. M. KERKER, "The Scattering of Light and Other Electromagnetic Radiation" (Academic, New York, 1969) Ch. 9.
37. J. CABANNES, *J. Physique Rad.* **6** (1920) 129.
38. C. CLAIRBORNE and B. CRIST, *J. Polym. Sci., Polym. Phys. Edn* **17** (1979) 719.
39. R. E. JUDD and B. CRIST, *J. Polym. Sci., Polym. Lett. Edn* **18** (1980) 719.
40. M. FUJIKI, T. KAINO and S. OIKAWA, *Polym. J.* **15** (1983) 693.
41. J. F. RUDD, *Polym. Lett.* **4** (1966) 929.
42. F. URBACH, *Phys. Rev.* **92** (1953) 1324.
43. D. A. PINNOW, T. C. RICH, F. W. OSTERMAYER and M. Di DOMENICO, *Appl. Phys. Lett.* **22** (1973) 527.
44. P. C. SCHULTZ, *J. Amer. Chem. Soc.* **57** (1974) 309.
45. W. A. GAMBLING, D. N. PAYNE, C. R. HAMMOND and S. R. NORMAN, *Proc. IEE* **123** (1976) 570.
46. R. D. MAURER, *ibid.* **123** (1976) 257.
47. W. KAYE, *Spectrochim. Acta* **6** (1954) 257.
48. S. FUJIMOTO, *SPIE Proc.* **799** (1987) Paper 23.
49. J. CONTI-RAMSDEN, R. M. GLEN and R. T. MURRAY, *ibid.* **799** (1987) Paper 21.
50. W. E. HANFORD and R. M. JOYCE, *J. Amer. Chem. Soc.* **68** (1946) 2082.
51. WESTERN ELECTRIC Co., U.K. Patent 1 389 263 (1973).
52. A. S. KENYON, R. C. GROSS and A. L. WURSTNER, *J. Polym. Sci.* **40** (1959) 159.
53. B. BOUTEVIN, Y. PIETRASANTA, G. RIGAL and A. ROUSSEAU, *Ann. Chim. Fr.* **9** (1984) 723.
54. T. KAINO, *Konbushi Ronbushu* **42** (1985) 257 (in Japanese).
55. J. M. SENIOR, "Optical Fiber Communications" (Prentice-Hall, London, 1985) Ch. 3.
56. R. M. GLEN, *Chemtronics* **1** (1986) 98.
57. D. MARCUSE, *Appl. Opt.* **18** (1979) 2073.
58. Y. OHTSUKA, T. SENGA and H. YASUDA, *Appl. Phys. Lett.* **25** (1974) 659.
59. Y. OHTSUKA, T. SUGANO and Y. TERAO, *Appl. Opt.* **20** (1981) 2319.
60. Y. OHTSUKA, Y. KOIKE and H. YAMAZAKI, *ibid.* **20** (1981) 280.
61. *Idem, ibid.* **20** (1981) 2726.
62. Y. KOIKE, Y. KIMOTO and H. YAMAZAKI, *ibid.* **21** (1982) 1057.
63. Y. OHTSUKA and Y. KOIKE, *Optics* **12** (1983) 470 (in Japanese).
64. Y. KOIKE, H. HATANAKA and Y. OHTSUKA, *Appl. Opt.* **23** (1984) 1779.
65. C. CLAIRBORNE and B. CRIST, *Coll. Polym. Sci.* **257** (1979) 457.
66. SUMITOMO CHEMICAL Co., European Patent Application 97 325 (1983).

Received 18 September
and accepted 22 September 1987